doi:10.20944/preprints202011.0517.v1

Article

Gas phase TiO_2 photosensitized mineralization of some VOCs: Mechanistic suggestions through a Langmuir-Hinshelwood kinetic approach

Marta Bettoni [1], Stefano Falcinelli [1,*], Cesare Rol [2], Marzio Rosi [1] and Giovanni Vittorio Sebastiani [1]

[1] Dipartimento di Ingegneria Civile ed Ambientale, Università di Perugia, Via G. Duranti 93, 06125 Perugia, Italy; marta.bettoni.mb@gmail.com; stefano.falcinelli@unipg.it; marzio.rosi@unipg.it; gvsebastiani@gmail.com

[2] Dipartimento di Chimica, Biologia e Biotecnologie, Università di Perugia, Via Elce di Sotto 8, 06123 Perugia, Italy; cesarepianista@gmail.com

* Correspondence: stefano.falcinelli@unipg.it; Tel.: +39-075-585-3862 (S.F.)

Abstract: A jointed experimental and theoretical investigation pointing out new insights about the microscopic mechanism of the VOCs (volatile organic compounds) photocatalytic elimination by TiO_2 has been done. Methane, hexane, isooctane, acetone and methanol have been photomineralized in a batch reactor. Values of K (adsorption constant on TiO_2) and k (mineralization rate constant) of the five VOCs (treating the kinetic data through a Langmuir- Hinshelwood approach) have been determined. Recorded K and k values and performed theoretical calculations allowed us to suggest the involvement of an electron transfer step between the VOC and the hole, $TiO_2(h^+)$, as the rate determining one.

Keywords: titanium dioxide; oxidation; photocatalysis; VOCs mineralization; Langmuir-Hinshelwood

---

0. How to Use This Template

The template details the sections that can be used in a manuscript. Note that each section has a corresponding style, which can be found in the 'Styles' menu of Word. Sections that are not mandatory are listed as such. The section titles given are for Articles. Review papers and other article types have a more flexible structure.

Remove this paragraph and start section numbering with 1. For any questions, please contact the editorial office of the journal or support@mdpi.com.

1. Introduction

The TiO_2 photosensitized mineralization of most VOCs (volatile organic compounds) as pollutants has been widely considered [1-9] principally due to its biological and chemical inertness, strong oxidizing power, low cost and long-time stability against photo- and chemical corrosion of this semiconductor.

The photochemical process is known to involve the VOC pre-adsorption at the sensitizer surface followed by the generation of hole/electron pairs into the semiconductor through the absorption of light with energy equal to or higher than the band-gap energy; the electrons reduce the atmospheric oxygen while the holes oxidize the VOC, directly (through an electron transfer process from the organic substrate to the hole) or indirectly (through the intervention of radicals HO· derived from the oxidation of adsorbed water by the hole) [10,11].

In current literature many authors have reported about the effect of TiO_2 properties on the gas phase photocatalytic efficiency while a minor number of papers concern the effect of the VOC structure on the adsorption at TiO_2 surface and on the reaction efficiency. In particular, the considered VOCs have been principally alkanes [12-17], chloroalkanes [12,18], chloroalkenes, [10,12,18], carbonyl derivatives [10,12,15,16,19], alcohols [10,12,18,19], ethers [12] and aromatic compounds [10,12].

Within the previous organic substrates, in this paper we have selected five VOCs (methane, hexane, isooctane, acetone and methanol) that, in our experimental conditions, are quantitatively mineralized to CO_2 and H_2O. In particular, the experiments have been carried out in a batch reactor (irradiation with high power external lamp through a Pyrex cap).

Preliminarily, in the first topic of this work (see Sect. 2.1), a series of different TiO_2 powders, prepared by a sol-gel method and annealed at different temperatures, have been considered. These powders show properties (such as crystalline form, crystallinity degree, crystal size, surface area, pore volume) that gradually change with the calcination temperature as demonstrated by previous investigations [20] using Brunauer, Emmett and Teller theory (BET), X-ray powder diffraction analysis (XRD) and thermogravimetric analysis (TG). These samples have been used to verify if the relative efficiency of two substrates with different polarity (hexane and acetone) is maintained changing the type of TiO_2 used. In particular, in this work the different TiO_2 powders have been used to realize a profile "TiO_2 efficiency vs. powder annealing temperature" in the presence of hexane as a non polar substrate at 600 ppm substrate concentration, evaluating the rate through a simplified Langmuir-Hinshelwood (LH) treatment, as apparent rate (k_a, as discussed in eq. 3, Sect. 2.1); these data have been compared with the same measurements previously performed for acetone as a polar substrate [20].

A second topic (see Sect. 2.2) that has been considered in this work involves the determination of the values of K and k for the above five substrates in the presence of TiO_2 P25, a very reactive commercial powder (see Sect. 3.1), changing the initial VOC concentration and treating the kinetic data with LH equation (see eq. 4 and Sect. 2.2).

The presented data allowed to obtain important mechanistic information about the considered substrates oxidation reactions. A careful analysis of the kinetic experimental evidences together with theoretical considerations (see below) highlights that the rate determining step in the reaction mechanism of the investigated photosensitive oxidations, is an electron transfer step ($RH \rightarrow RH^{+\cdot} + e^-$) instead of a possible competitive homolytic process ($RH\cdot \rightarrow R\cdot + H\cdot$). To obtain this information, which constitutes the novelty of our work, a jointed experimental and theoretical investigation has been done: i) chemical kinetics experiments via a Langhmuir-Hinshelwood approach for the determination of either K (the adsorption constant on TiO_2) and k (the mineralization rate constant) using five VOCs (methanol, acetone, iso-octane, hexane, and methane) have been performed; ii) computational analysis through the optimization of the geometry of the involved neutral and the corresponding radical cations species has been done and the ionization potentials of the considered substrates, both in the absence and in the presence of water molecules, always present at the semiconductor surface (see Sect. 2.3), were determined. The expertise of our research group during last decade on the experimental and theoretical characterization of the chemical behaviour of ionic and radical species in gas phase [21,22] and in heterogeneous/homogeneous catalytic processes [23,24] has been used. This type of kinetic experiments coupled with theoretical investigations performed with a high level of accuracy have important applications in the development of innovative photocatalytic reactors for the treatment of gaseous environmental pollutants and for industrial purposes.

2. Results and Discussion

2.1. Photo-oxidation of hexane with different synthetic TiO_2 powders

It is useful to discuss as first about the topic relative to the data of photocatalytic efficiency obtained in the presence of different synthetic powders, considering hexane (a non polar VOC) as substrate; this allows to compare the behavior of this substrate with that of a previously studied VOC, acetone (a polar substrate) [20].

As previously reported [20,25], the considered powders have been prepared by hydrolysis of TTIP and by subsequent calcination at different temperatures. In this way, various powders with

doi:10.20944/preprints202011.0517.v1

different properties, such as crystalline form (anatase and/or rutile), crystallinity degree, crystal size, surface area and pore volume [20,25], have been synthesized. The discussion relative to the change of each of the above properties as a function of the calcination temperature of the different powders have been reported in previous articles [20,25].

The gas phase TiO_2 photosensitized oxidation has been carried out in a thermostated static reactor (28±3°C, at constant humidity and oxygen concentration). The data relative to the reaction stoichiometry, as residual hexane and produced CO_2, are reported in Section 2.2 and support the complete mineralization of the substrate. The most used equation that allows to obtain the adsorption equilibrium constant (K) and the reaction rate constant (k) from kinetic data is the LH equation (Sect. 2.1) [3,5].

The hexane photocatalytic degradation follows the LH equation [5] (see eq. 1 below, where r is the rate, k is the true rate constant, K is the adsorption constant of the substrate on TiO2 and C is the substrate concentration).

$$r = kKC/(1+KC) \tag{1}$$

As the considered initial concentration of hexane (600 ppm: the same concentration value previously used in our laboratory in the case of similar kinetic experiments involving acetone [20]) is low, we have utilized a simplified LH equation (see eq. 2 below) where k_a, the apparent rate constant, can represent a quantitative kinetic measure of the powder relative efficiency (see for example ref. 26).

$$r = kKC = k_aC \tag{2}$$

The integrated form of the rate equation, as the function of the time t, is reported in eq. 3, where C_0 is the substrate starting concentration.

$$\ln (C_0/C) = \ln [100/(100 - \%CO_2)] = k_at \tag{3}$$

In this way, from the plots in Fig 1 we have obtained a series of kinetic linear correlations for the different synthetic powders (see Table 1 where R is the correlation coefficient).

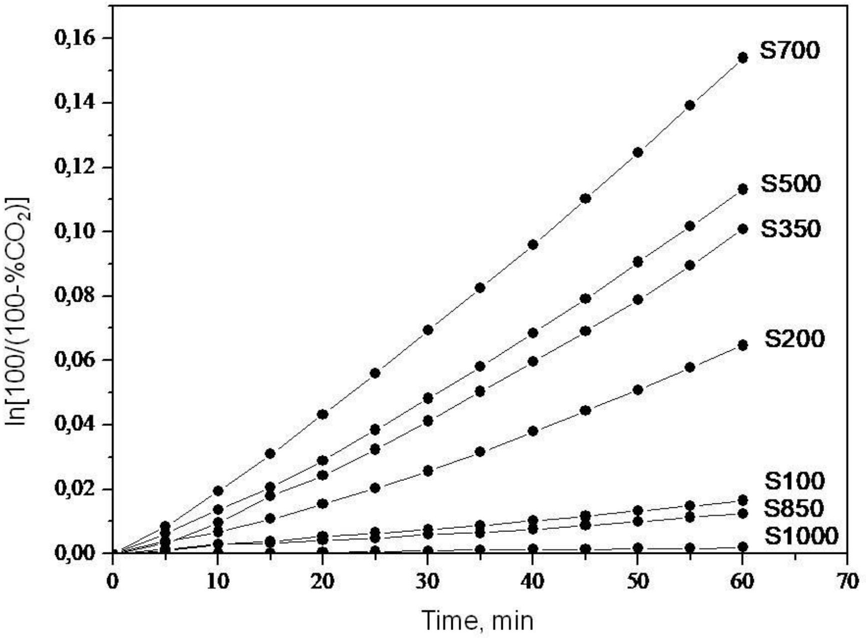

Figure 1. Langmuir-Hinshelwood kinetic plots (see eq. 3) based on CO_2 produced from the photo-oxidation of hexane (600 ppm) sensitized by synthetic TiO_2 samples (calcined from 100°C, S100, to 1000°C, S1000).

Table 1. Apparent rate constants (k_a) from the Langmuir-Hinshelwood treatment (see eq. 3) based on CO_2 produced from the TiO_2 samples photosensitized oxidation of hexane (concentration: 600 ppm; reaction time: 1h). R is the correlation coefficient.

Sample	$k_a \times 10^3$, min^{-1}	R
S100	0.260	0.9988
S200	0.990	0.9907
S350	1.500	0.9916
S500	1.700	0.9947
S700	2.400	0.9973
S850	0.200	0.9972
S1000	0.032	0.9908

In Fig 2 are reported the values of the slopes (k_a) obtained until one hour of reaction (starting from 600 ppm of hexane and at 12±3% relative humidity (RH) vs. the TiO_2 annealing temperatures. As observed with acetone [20], the efficiency increases (ca. 10 times) from 100°C up to 700°C in the hexane profile (see Fig 2) and this behavior could be attributed to the crystallinity increase of the anatase structure. Otherwise, for both substrates the efficiency decrease (ca. 20 times) from 700°C to 1000°C could be ascribed to a gradual change of the crystal form from anatase (more reactive) to rutile (less reactive). A first observation is that the selection of the most efficient TiO_2 (calcinated at 700°C for both substrates) and the less efficient one (calcinated at 1000°C for both substrates) is independent from the substrate polarity. Another observation could be that the relative efficiency of the two substrates is maintained independently from the type of selected TiO_2; in fact, acetone is ca. 2-3 times more reactive than hexane with all the synthesized TiO_2 powders.

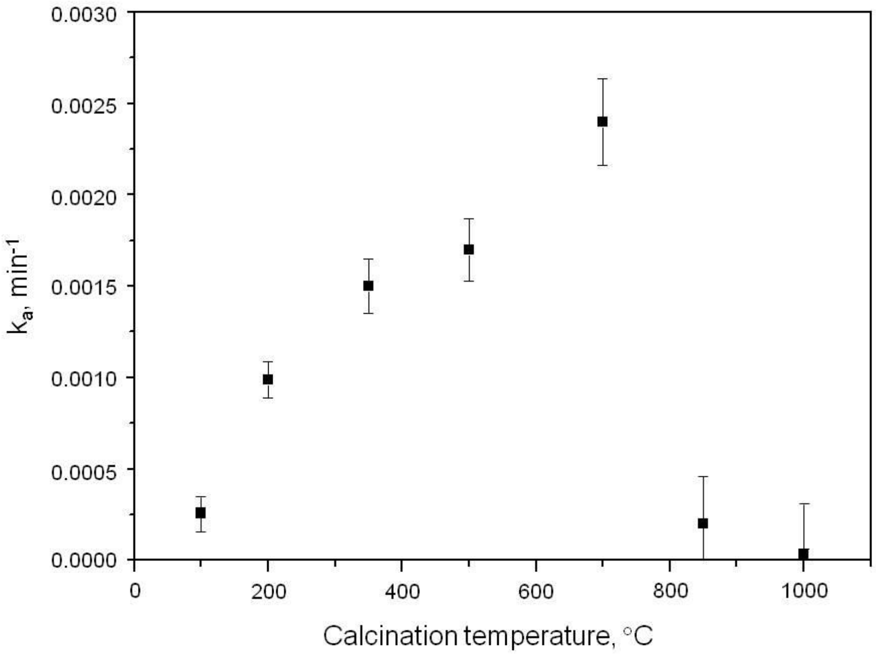

Figure 2. The dependence of the apparent kinetic constants (k_a in eq. 3) from the calcination temperature of TiO_2 powders.

2.2. Photo-oxidation of methane, hexane, isooctane, acetone and methanol with TiO_2 P25

In this paragraph we consider the LH equation (eq. 1) in the form of eq. 4 below, where $r_\circ$ is the starting rate and $C_\circ$ is the starting concentration (see for example ref. 10), to obtain the values of k and K of the considered substrates.

Preprints (www.preprints.org) | NOT PEER-REVIEWED | Posted: 19 November 2020 doi:10.20944/preprints202011.0517.v1

$$1/r_o = 1/kK \; 1/C_o + 1/k \qquad (4)$$

Preliminarily, the reaction stoichiometry for the considered substrates has been verified by us for acetone (as reported in ref. 20), for hexane in this work (after 1 h reaction, starting from 600 ppm of hexane and at 12±5% RH, 250 ppm of hexane residue and 1920 ppm of CO_2 are recovered) or on the base of the literature [13-15,18,27,28].

Another preliminary observation is that the used cap material (Pyrex) almost completely avoids the direct photolysis of the substrate, as verified by blank experiments performed in the absence of TiO_2. It must be observed that the use of Pyrex as light filter is an experimental reaction condition which is crucial to study exclusively the TiO_2 sensitized photooxidation mechanism, even if this comes at the expense of substrates conversion. In particular, in these experimental conditions the less reactive substrate (methane) cannot be quantitatively studied: in fact, starting from 600 ppm of substrate, 23, 35 and 47 ppm of CO_2 are obtained, after 1, 2 and 3 h respectively, that represent a very little amount of CO_2, comparable with the results obtained in the absence of TiO_2 (7, 13 and 22 ppm). As shown in Figures 3-6, with each substrate (hexane, isooctane, acetone and methanol) the slope (r from the linear correlation between [CO_2] and t) remains nearly constant until 1h of reaction ($R \geq 0.99$) for each considered C_o and therefore r_o can be identified with r. In the photocatalytic degradation kinetic data of Figures 3-6, the use of slightly different initial VOCs concentrations is due to the difficulty of manually sampling exactly the same concentration value by the operator.

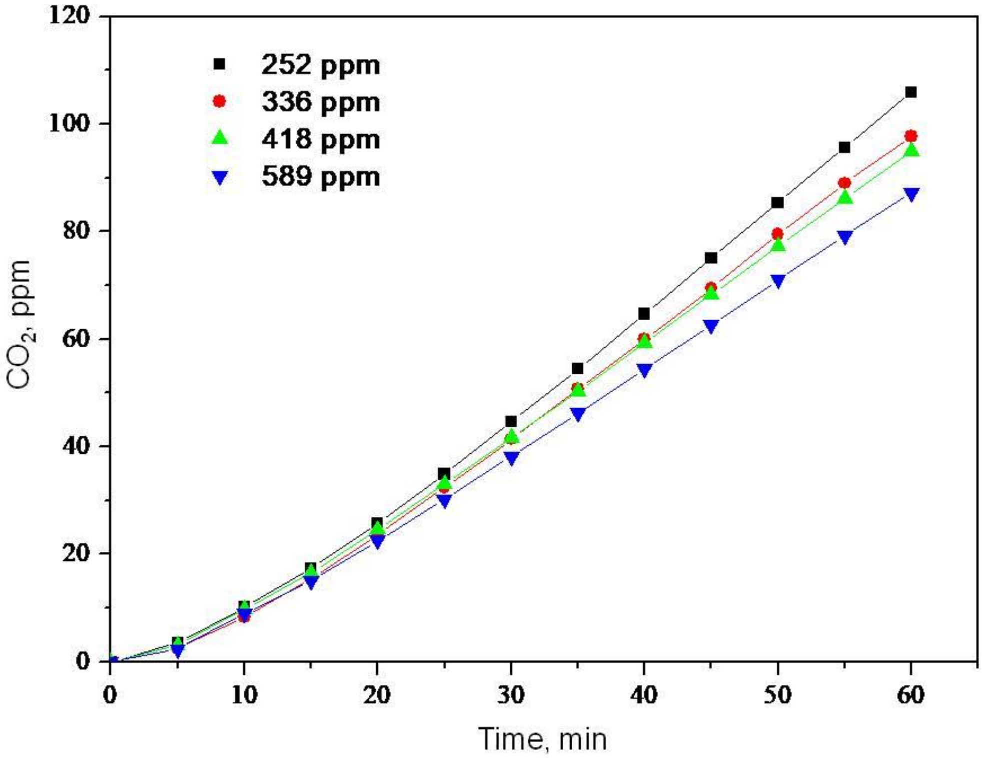

Figure 3. Photocatalytic degradation of hexane (as CO_2 produced) at different initial concentration of the substrate. TiO_2 (P25, Degussa) commercial powder is used.

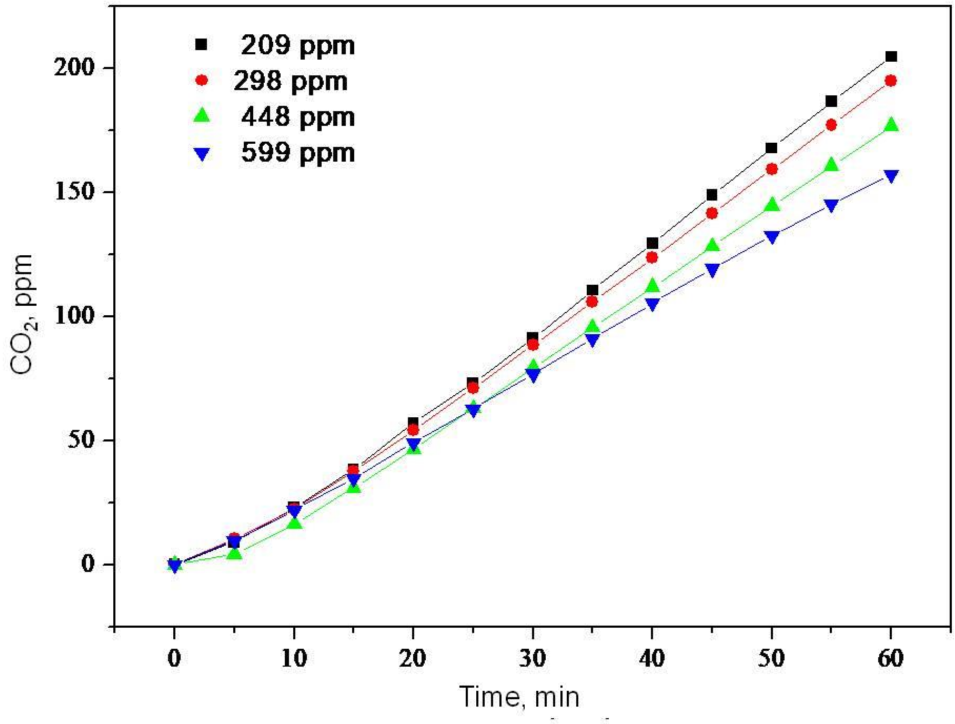

Figure 4. Photocatalytic degradation of acetone (as CO_2 produced) determined at different initial concentration of the substrate. TiO_2 (P25, Degussa) commercial powder is used.

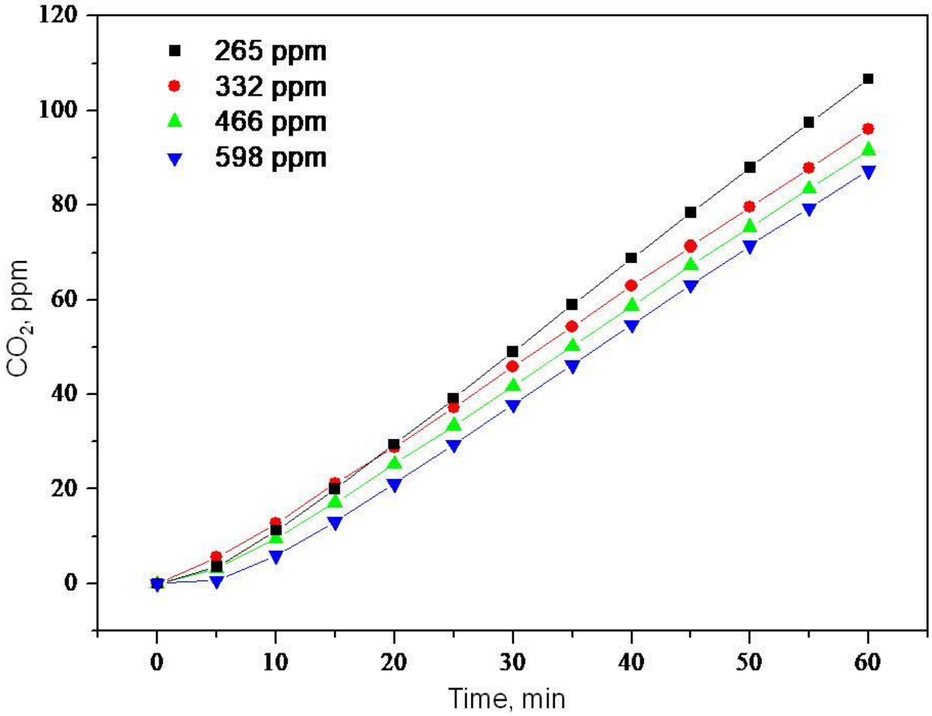

Figure 5. Photocatalytic degradation of isooctane (as CO_2 produced) determined at different initial concentration of the substrate. TiO_2 (P25, Degussa) commercial powder is used.

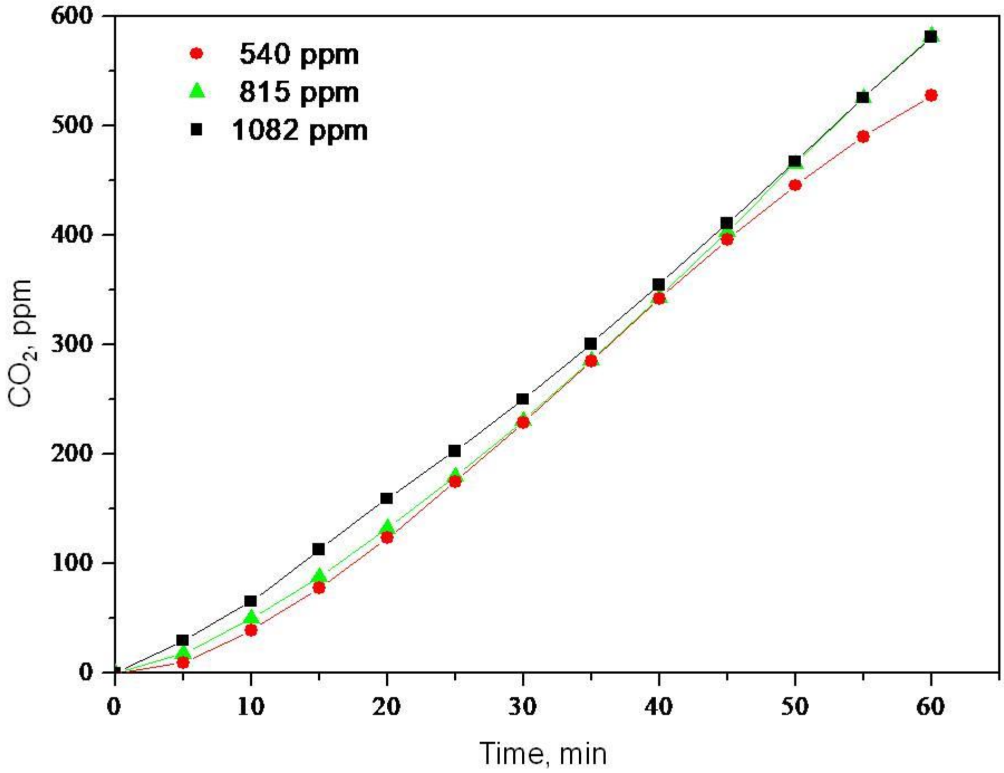

Figure 6. Photocatalytic degradation of methanol (as CO_2 produced) determined at different initial concentration of the substrate. TiO_2 (P25, Degussa) commercial powder is used. In this case, only three initial substrate concentration values were analyzed owing to the difficulties encountered in manual sampling due to the very high vapor pressure of the methanol.

In the kinetic data reported in Fig. 6, since the photocatalytic degradation of methanol is characterized by the higher reaction rate compared to the other VOCs studied, as shown in Table 2, the final CO_2 concentrations detected are considerably higher than in the other cases.

In Fig 7 are reported the plots (relative to the four substrates) of $1/r_0$ vs. $1/C_0$ that allow to obtain the values of k and K for each substrate. The values of the constants are reported in Table 2.

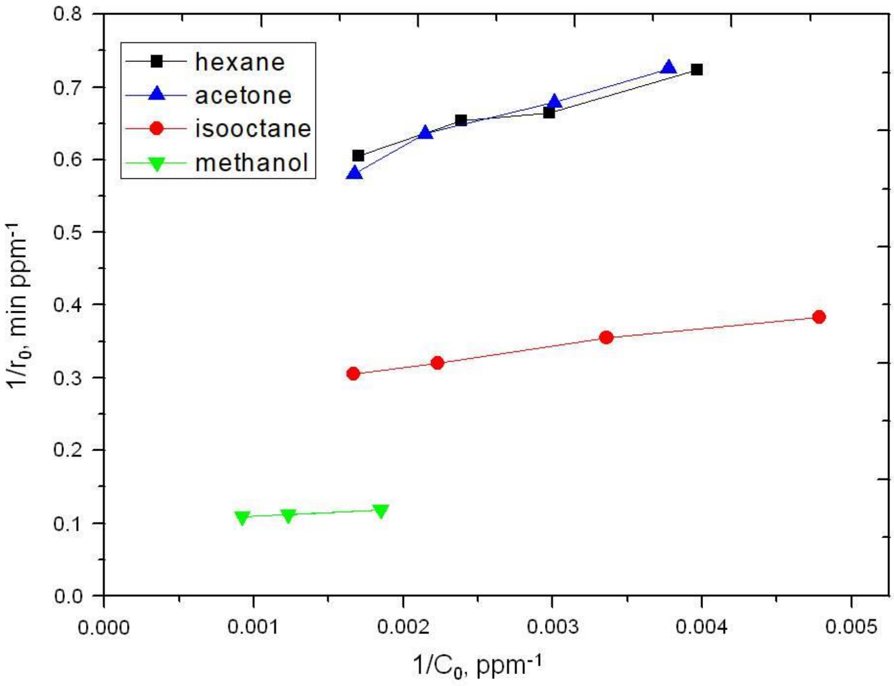

Figure 7. Langmuir–Hinshelwood plots (eq. 4) relative to hexane (square), isooctane (triangle up), acetone (circle) and methanol (triangle down).

Table 2. Langmuir-Hinshelwood parameters (k and K) relative to the photosensitized oxidation of hexane, acetone, isooctane and methanol.

Substrate	k, ppm min^{-1}	K×10^{2}, ppm^{-1}	kK×10^{2}, min^{-1}
Hexane	1.9	1.05	2.0
Acetone	3.8	1.05	4.0
Isooctane	2.1	0.74	1.5
Methanol	9.9	1.11	11.0

Before discussing the results in Table 2, it must be noted that other authors have determined, through the LH treatment, k and K values relative to, at most, two substrates but in our knowledge no author has already used the comparison of these data to deduce mechanistic information [10,12,14]. In fact, the experimental conditions used in these works don't allow to suggest a mechanism exclusively related to the TiO_2 photosensitized oxidation as in these conditions the substrates also undergo competitive direct photolysis [10,14] or thermal reaction [12].

As concerns the K values in Table 2, it is evident that they are similar with a significative contribute probably given by Van der Waals (VdW) interactions. As a confirmation, between the two alkanes (hexane and isooctane), the one with a lower contact surface (isooctane) is slightly less adsorbed (lower K).

To tentatively evaluate also the relative efficiency of methane (not inserted in Table 2 due to its low reaction rate) it can be considered the amount of CO_2 produced at the same reaction time (for example 1h) from the same amount of substrate (for example 600 ppm of methane and hexane). In this way methane (see above data in this paragraph) is at least four times less efficient than n-hexane (see Fig 3). The undetectable reactivity (Kk) of methane (not present in Table 2), that presents a minimal contact surface (since a lower VdW interaction), suggests a significant contribution of a very low K to the Kk (efficiency) value of this hydrocarbon.

As concerns the two polar compounds, acetone and methanol, the K values are similar to that of hexane, a non polar compound, probably because the minor contribute of the VdW interactions (due to a lower contact surface) could be compensated by a dipole-dipole interaction, for acetone, and dipole-dipole interaction via hydrogen bond, for methanol, with water always present at the TiO_2 surface. As for the k values in Table 2 it can be observed that the non polar substrates, hexane and iso-octane, are less reactive than the polar ones, acetone and methanol, suggesting an electron transfer rate determining step, $RH + TiO_2(h^+) \rightarrow RH^{+\cdot} + TiO_2$, in the reaction mechanism, as observed in liquid phase (see references cited in ref. 20). In fact, the radical cations deriving from the polar compounds are more stable than those from the non polar ones. The exclusion of an homolytic process, $RH + OH\cdot \rightarrow R\cdot + H_2O$, as rate determining step, is also supported by the nearly same reactivity of hexane and iso-octane. In fact, considering the relative stability of the correspondingly produced radicals in the above step (the tertiary radical obtained from a hydrogen extraction from iso-octane is more stable than anyone formed from hexane) iso-octane should be more reactive than hexane.

2.3. Evaluation of ionization potentials

In order to evaluate the operation of an electron transfer mechanism, the ionization potentials (IPs) of methanol, acetone, n-hexane and methane have been calculated, optimizing the geometry of the neutral molecules and of the corresponding positive ions (that is the corresponding radical cations) at B3LYP/aug-cc-pVTZ level. At the optimized structures we performed a single point calculation at CCSD(T)/aug-cc-pVTZ level in order to have a more accurate energy value. The computed IPs are reported in Table 3, together with the experimental values. [29].

Table 3. Ionization potential (eV) computed at the CCSD(T)/aug-cc-pVTZ//B3LYP/aug-cc-pVTZ level of theory at 298.15 K for the investigated molecules. Experimental values [29] are reported for comparison.

Substance	IP(eV)		IP(eV) in the presence of H_2O	IP(eV) in the presence of 2 H_2O
	CCSD(T)	Experiment	CCSD(T)	CCSD(T)
Methanol	10.81	10.84	9.63	9.17
Acetone	9.65	9.703	9.54	---
n-Hexane	9.96	10.13	---	---
Isooctane	---	9.89	---	---
Methane	12.66	12.61	---	---

We can notice that the CCSD(T) computed values are in good agreement with the experimental values, the discrepancy being 0.03, 0.05, 0.05 and 0.17 eV for methanol, acetone, methane, and n-hexane, respectively. It can be observed that the relative experimental values for acetone, n-hexane, isooctane and methane are in line with an electron transfer step as rate determining ($k_{acetone} > k_{hexane} \approx k_{iso\text{-}octane} > k_{methane}$). On the contrary, the IP value of methanol (both the experimental and the computational one) is much higher than expected: assuming the operation of an electron transfer mechanism, the above value should have been the lowest of the series.

We suggest that a possible justification of this apparent anomaly could be the presence of water molecules, always present at the TiO_2 surface, that can interact with polar molecules (through dipole-dipole interactions with acetone or dipole-dipole via hydrogen bond with methanol). Therefore, for methanol and acetone we computed the IPs also in the presence of one water molecule. From the optimized geometries reported in Fig 8 we can notice that there is a strong interaction of the water molecule with ionized methanol.

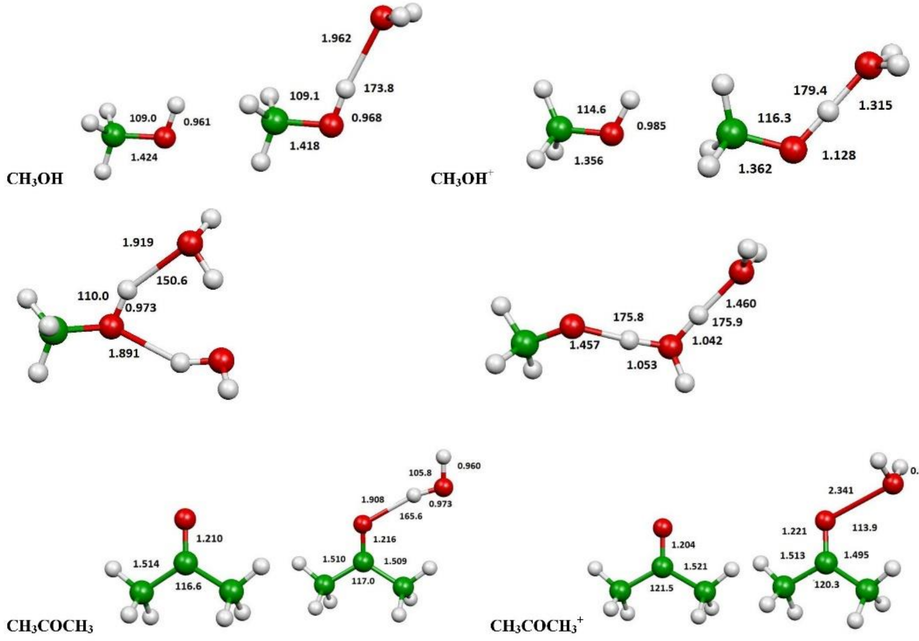

Figure 8. B3LYP optimized geometries (Å, and °) of the gas phase methanol and acetone neutrals and radical cations with and without surrounding water molecules (see text).

The $H_2O—HOCH_3$ distance, which is 1.962 Å in the neutral system, becomes 1.315 Å in the ionized complex; moreover, the methanol O—H bond length increases from 0.968 Å to 1.128 Å and the O—H—O angle, which is 173.8° in the neutral system, becomes 179.4° in the ionized one. The geometry of the complex $[CH_3OH^{\cdots}OH_2]^{+\cdot}$suggests, therefore, the presence of an hydrogen bond between methanol radical cation and water molecule. This is confirmed also by the Mulliken charges, reported in Fig 9 for methanol and acetone, which shows a charge transfer of 0.29 e from the water molecule to the ionized methanol molecule.

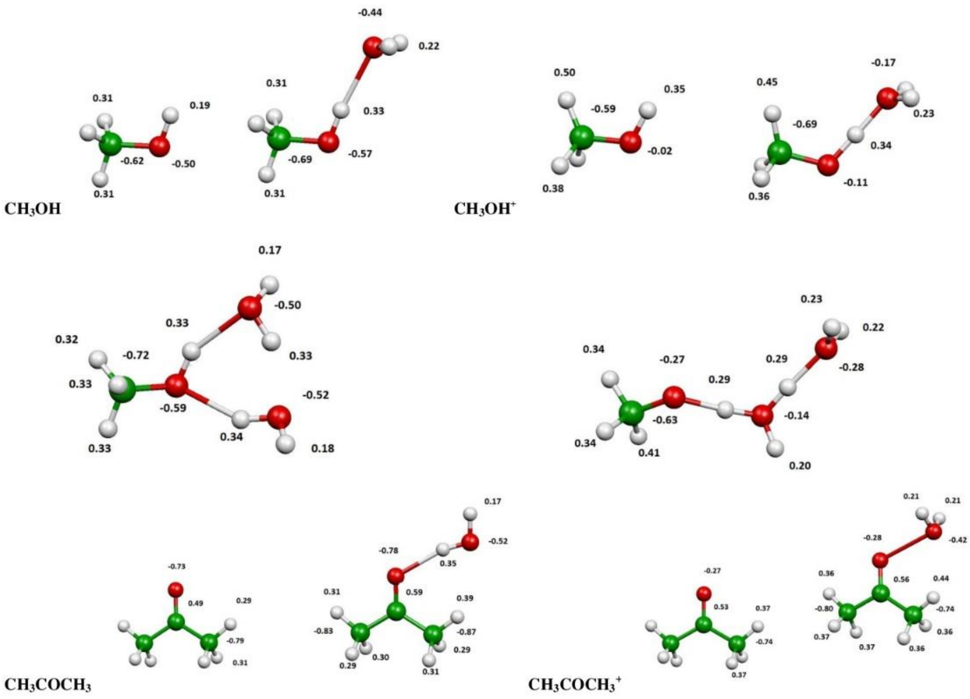

Figure 9. Calculated Mulliken charges for methanol and acetone neutrals and radical cations with and without surrounding water molecules (see text).

This interaction decreases the energy of the ionized species to a greater extent with respect to the neutral species when one water molecule is present. The consequence is a smaller value of the IP due to the presence of one water molecule (9.63 eV instead of 10.81 eV, as we can see from Table 3). Since the influence of water on the ionization potential of methanol is very strong, we investigated also the effect of a second molecule of water. From the optimized geometries shown in Fig 8, we can notice that in the presence of a second molecule of water we have a transfer of a proton from $CH_3OH^{+\cdot}$ to H_2O and the system is best described as $CH_3O^{\cdot}$---H_3O^{+}---H_2O.

As we can see from Table 3, the ionization potential of methanol in the presence of two molecules of water is 9.17 eV (the lowest IP of the series), therefore the IP decreases by 0.46 eV with respect to the presence of only one molecule of water. The total decrease of the IP of methanol due to the presence of two water molecules therefore is 1.64 eV.

A water molecule does not seem to interact strongly with acetone (both neutral and ionized) as we can see from the optimized structures reported in Fig 8. Actually we have a slightly stronger interaction with the neutral molecule (the $(CH_3)_2CO—HOH$ distance is 1.908 Å) than with the ionized one the $[(CH_3)_2CO—OH_2\ ]^{+\cdot}$distance is 2.341 Å). For this reason, the IP of acetone does not change significantly in the presence of one water molecule (9.54 eV instead of 9.65 eV). Also, the Mulliken charges reported in Fig 9 show that the interaction of acetone with water is small, as we can notice from the lack of charge transfer from water to acetone.

3. Materials and Methods

3.1. Materials

Commercial samples of Titanium(IV)tetraisopropoxide (TTIP, Aldrich, 97%), TiO_2 (P25, Degussa), isopropanol (IP, Carlo Erba, 99.7%), acetone (Aldrich, 99%), hexane (Aldrich, 97%), isooctane (Riedel-de Haen, 99%), methanol (Carlo Erba, 99,9%), gas mixture (O_2, 20% and N_2, 80%, Air Liquide) have been used. The gaseous mixture containing 600 ppm of CH_4 in a N_2+O_2 mixture with a composition 80:20 was supplied by Air Liquide.

3.2. Synthesis of TiO_2 powders

A complete description of the synthesis and characterization of the used TiO_2 powders is already published [20] and here is given only a brief summary of the procedure. By magnetic stirring at room temperature 12 ml of TTIP were added to 500 ml of IP, and 2500 ml of Milli-Q water were then added slowly to the solution which was vigorously stirred for 24 hours in a closed flask. The white precipitate dispersed in the solvent was filtered and washed with Milli-Q water, and the white residue was dried (in an oven) and then grinded by a ceramic mortar. The derived particles were thermally treated for 1 h at 100, 200, 350, 500, 700, 850 and 1000 °C (a temperature gradient of 3°C/min has been used to reach each temperature value) [20].

3.3. Experimental apparatus

A cylindrical Pyrex glass static reactor (diameter = 29 cm, highness = 40 cm, volume = 11 l), equipped with an optical window (Pyrex, thickness =1 cm, diameter = 24 cm) and an o-ring with a metallic flange allowing hermetic seal, was used in the experiment. The reactor, already used in previous investigations, is described in detail elsewhere [20]. It is thermostated at 28±3 °C by water cooling and it has five connections: one is used for a fan (allowing the homogeneity of the gas reaction mixture during the experiment); a further connection allows the insertion of the gaseous reaction mixture (N_2/O_2) inside the reactor; additional connections are used for the introduction of liquid reagents by a syringe and for two electrical contacts. The first one is for a gas sensor Delta Ohm HD37B17D (used to monitoring in continuous the CO_2 concentration, the relative humidity and the internal temperature), while the second is for a manometer Delta Ohm HD2304 (used to measure the pressure inside the reactor).

3.4. Photodegradation of methane, hexane, isooctane, acetone and methanol in the presence of TiO_2

Inside the reaction chamber, the synthetic TiO_2 powder (2g) or TiO2 P25 (1g) was inserted to completely cover the internal surface of a Petri plate (diameter = 10 cm) placed on a Teflon support. Successively, the Pyrex cap was hermetically sealed, the reactor was vacuum (0.008 bar) degassed and ca. 600 ppm of the liquid reagent were inserted by a syringe. Then the pressure inside the reactor was increased (1.0 bar) adding the O_2/N_2 gas mixture. In the case of methane, the commercial mixture was used at 1.0 bar pressure. The apparatus was left for 1 h in the dark and then was externally irradiated by a 500 W high pressure mercury lamp (Helios Italquartz; the wavelength range of this polychromatic lamp through the Pyrex cap is in the range 300-580 nm) situated at 30 cm over the reaction chamber (the irradiation received by the photo-catalyst inside the reactor, measured by a radiometer, was 22 mW/m^2). The synthetic photocatalysts show light adsorption at wavelenghts < 580 nm. In the presence of the Pyrex cap of the glass reactor, this range becomes nearly 300-580 nm, a range in which all the synthetized TiO_2 samples adsorb the UV-vis radiation (see for example UV-vis DRS of samples prepared in the same way in ref. [30]).

3.5. Product analysis

Since in our case the only products of the photodegradation reactions of the simple VOCs studied are carbon dioxide and water in stoichiometric quantities, we have quantitatively determined the CO_2 formed. The analysis of the produced CO_2 was carried out by the gas sensor Delta Ohm HD37B17D through an IR cell. The analysis of the unreacted hexane was carried out quantitatively by the gas-chromatograph Varian 3900 with FID detector, using a CP-WAX 57CB capillary column.

3.6. Computational evaluation of ionization potentials

In order to evaluate the ionization potentials of methanol, acetone, and n-hexane we optimized the geometry of the neutral molecules and the corresponding radical cations at the B3LYP [31,32] level of theory in conjunction with the correlation consistent valence polarized set aug-cc-pVTZ [33,34], as we have already done for different systems [35-37]. At the same level of theory, we have computed the harmonic vibrational frequencies. The energy of the stationary points was computed then at the higher level of calculation CCSD(T) [38-40] using the same basis set aug-cc-pVTZ. The CCSD(T) energies were corrected to 298.15 K by adding the zero point energy correction and the thermal correction computed using the scaled harmonic vibrational frequencies evaluated at B3LYP/aug-cc-pVTZ level. The geometry of methanol and acetone was optimized also in the presence of one molecule of water in order to check the effect of this molecule on computed ionization potentials. For methanol we considered also the effect of the presence of a second molecule of water on its ionization potential. All calculations were performed using Gaussian 09 [41] while the analysis of the vibrational frequencies was performed using Molekel [42,43].

4. Conclusions

In the present paper we performed a jointed experimental and theoretical investigation on TiO_2 catalytic elimination of some VOCs environmental pollutants, pointing out new insights about the microscopic mechanism of the photocatalytic mineralization of five VOCs by TiO_2. By experiments we were able to verify that the relative efficiency of acetone and hexane, as substrates having different polarity, for direct photolysis is maintained using TiO_2 powders with different properties (crystalline form, degree and size, surface area and pore volume). Furthermore, we have conducted chemical kinetics experiments via a Langhmuir-Hinshelwood approach for the determination of either K (the adsorption constant on TiO_2) and k (the mineralization rate constant) using five VOCs (methanol, acetone, iso-octane, hexane, and methane). The recorded rate constant data showed that the non-polar molecules (hexane and iso-octane) are less reactive than the polar ones (acetone and methanol). These experimental data, together with a computational analysis of a high level of accuracy within our innovative approach, highlighted that the rate determining step in the reaction mechanism of the investigated photosensitive oxidations, should be an electron transfer step ($RH \rightarrow RH^{+\cdot} + e^-$) instead of a possible competitive homolytic process ($RH \rightarrow R\cdot + H\cdot$). Such experimental evidences are corroborated by our performed theoretical calculations concerning geometry and energetic stability of both neutral and cationic species of the investigated VOCs. Using the B3LYP level of theory coupled with the correlation consistent valence polarized set aug-cc-pVTZ, we determined the ionization potentials for used VOCs in presence of water molecules, since water is always present at the TiO_2 surface strongly interacting via dipole-dipole interactions with polar molecules as acetone and methanol. The performed computational analysis demonstrated that in the case of methanol (the most reactive VOC among those investigated in the present work) the presence of a hydrogen bond between the radical cation and the surrounding water molecules strongly stabilizes such hydrated radical cation respect to the case of isolated methanol. This causes a considerable decrease in the ionization potential of methanol when it is surrounded by two water molecules (in this case the IP is ~1.64 eV lower that the case of isolated methanol) justifying its stronger reactivity in photosensitive oxidations.

Finally, this work with its mechanistic implications on basic chemistry provides important evidences in the development of an innovative semiclassical model capable of fully describing the quantum state resolved reaction dynamics of prototype oxidation processes such as the chemiionization reactions [44,45].

Author Contributions: For research articles with several authors, a short paragraph specifying their individual contributions must be provided. The following statements should be used "Conceptualization and methodology, S.F., C.R., M.R. and G.V.S. software and theoretical calculations, M.R.; formal analysis, C.R. and G.V.S.; investigation and data curation, M.B.; writing—original draft preparation, M.B., S.F., C.R., M.R. and

G.V.S.; writing—review and editing, S.F., C.R., M.R. and G.V.S. All authors have read and agreed to the published version of the manuscript.

Funding: This research was funded by FONDAZIONE CASSA DI RISPARMIO DI PERUGIA, Italian MIUR and University of Perugia (Italy) within the program "Dipartimenti di Eccellenza 2018-2022".

Conflicts of Interest: The authors declare no conflict of interest. The funders had no role in the design of the study; in the collection, analyses, or interpretation of data; in the writing of the manuscript, or in the decision to publish the results.

References

1. Shayegan, Z.; Lee, C.S.; Haghighat, F. TiO_2 photocatalyst for removal of volatile organic compounds in gas phase – A review. *Chem. Eng. J.* **2018**, *334*, 2408-2439.
2. Verbruggen, S.W. TiO_2 photocatalysis for the degradation of pollutants in gas phase: From morphological design to plasmonic enhancement. *J. Photochem Photobiol. C: Photochem. Rev.* **2015**, *24*, 64-82.
3. Paz, Y. Application of TiO_2 photocatalysis for air treatment: Patents' overview. *Appl. Catal. B: Environmental* **2010**, *99*, 448-460.
4. Tseng, T.K.; Lin, Y.S.; Chen, Y.J.; Chu, H. A Review of Photocatalysts Prepared by Sol-Gel Method for VOCs Removal. *Int. J. Mol. Sci.* **2010**, *11*, 2336-2361.
5. Mo, J.; Zhang, Y.; Xu, Q.; Lamson, J.J.; Zhao, R. Photocatalytic purification of volatile organic compounds in indoor air: A literature review. *Atmos. Environ.* **2009**, *43*, 2229-2246.
6. Gaya, U.I.; Abdullah, A.H. Heterogeneous photocatalytic degradation of organic contaminants over titanium dioxide: A review of fundamentals, progress and problems. *J. Photochem Photobiol. C* **2008**, *9*, 1-12.
7. Wang, S.; Ang, H.M.; Tade, M.O. Volatile organic compounds in indoor environment and photocatalytic oxidation: State of the art. *Eviron. Int.* **2007**, *33*, 694-705.
8. Zhao, J.; Yang, X. Photocatalytic oxidation for indoor air purification: a literature review. *Build. Environ.* **2003**, *8*, 645-654.
9. Peral, J.; Domènech, X.; Ollis, D.F. Heterogeneous Photocatalysis for Purification, Decontamination and Deodorization of Air. *J. Chem. T echnol. Biotechnol.* **1997**, *70*, 117-140.
10. Kim, S.B.; Hong, S.C. Kinetic study for photocatalytic degradation of volatile organic compounds in air using thin film TiO_2 photocatalyst *Appl. Catal. B:Environmental* **2002**, *35*, 305-315.
11. Hoffmann, M.R.; Martin, S.T.; Choi, W.; Bahnemann, D.W. Environmental applications of semiconductor photocatalysis. *Chem. Rev.* **1995**, *95*, 69-96.
12. Alberici, R.M.; Jardim, W.F. Photocatalytic destruction of VOCs in the gas-phase using titanium dioxide. *Appl. Catal. B: Environmental* **1997**, *14*, 55-68.
13. Deng, X.; Yue, Y.; Gao, Z. Gas-phase photo-oxidation of organic compounds over nanosized TiO_2 photocatalysts by various preparations. *Appl. Catal. B: Environmental* **2002**, *39*, 135-147.
14. Boulamanti, A.K.; Philippopoulos, C.J. Photocatalytic degradation of C_5–C_7 alkanes in the gas–phase. *Atmos. Environ.* **2009**, *43*, 3168-3174.
15. Stengl, V.; Houskova, V.; Bakardjieva, S.; Murafa, N. Photocatalytic degradation of acetone and butane on mesoporous titania layers. *New J. Chem.* **2010**, *34*, 1999-2005.
16. Zorn, M.E.; Hay, S.O.; Anderson, M.A. Effect of molecular functionality on the photocatalytic oxidation of gas-phase mixtures. *Appl. Catal. B: Environmental* **2010**, *99*, 420-427.
17. Moulis, F.; Krysa, J. Photocatalytic degradation of several VOCs (n-hexane, n-butyl acetate and toluene) on TiO_2 layer in a closed-loop reactor. *Catal. Today* **2013**, *209*, 153-158.
18. Lichtin, N.N.; Avudaithai, M. TiO_2-Photocatalyzed Oxidative Degradation of CH_3CN, CH_3OH, C_2HCl_3, and CH_2Cl_2 Supplied as Vapors and in Aqueous Solution under Similar Conditions. *Environ. Sci. Technol.* **1996**, *30*, 2014-2020.
19. Neti, N.R.; Parmar, G.R.; Bakardjieva, S.; Subrt, J. Thick film titania on glass supports for vapour phase photocatalytic degradation of toluene, acetone, and ethanol. *Chem. Eng. J.* **2010**, *163*, 219-229.
20. Bettoni, M.; Candori, P.; Falcinelli, S.; Marmottini, F.; Meniconi, S.; Rol, C.; Sebastiani, G.V. Gas phase photocatalytic efficiency of TiO_2 powders evaluated by acetone photodegradation. *J. Photochem Photobiol. A: Chem.* **2013**, *268*, 1-6.
21. Skouteris, D.; Balucani, N.; Faginas-Lago, N.; Falcinelli, S.; Rosi, M. Dimerization of methanimine and its charged species in the atmosphere of Titan and interstellar/cometary ice analogs. *A&A* **2015**, *584*, A76.

22. Falcinelli, S.; Rosi, M.; Cavalli, S.; Pirani, F.; Vecchiocattivi, F. Stereoselectivity in Autoionization Reactions of Hydrogenated Molecules by Metastable Noble Gas Atoms: The Role of Electronic Couplings. *Chem. Eur. J.* **2016**, *22*, 12518-12526.
23. Falcinelli, S.; Capriccioli, A.; Pirani, F.; Vecchiocattivi, F.; Stranges, S.; Martì, C.; Nicoziani, A.; Topini, E.; Laganà, A Methane production by CO_2 hydrogenation reaction with and without solid phase catalysis. *Fuel* **2017**, *209*, 802-811.
24. Falcinelli, S. Fuel production from waste CO_2 using renewable energies. *Catal. Today* **2020**, *348*, 95-101.
25. Bettoni, M.; Candori, P.; Marmottini, F.; Perenze, N.; Rol, C.; Sebastiani, G. V.; Vecchiocattivi, F. Photocatalytic Activity in CH_3CN Related to the Surface Properties of TiO_2 Powders Prepared by Sol-Gel Method *Int. J. Photoenergy* **2009**, *2009*, ID905987.
26. Yu, J.C.; Yu, J.; Zhang, L.; Ho, W. Enhancing effects of water content and ultrasonic irradiation on the photocatalytic activity of nano-sized TiO_2 powders. *J. Photochem. Photobiol. A: Chem.* **2002**, *148*, 263-271.
27. Yu, H.; Yu, J.; Cheng, B. Photocatalytic activity of the calcined H-titanate nanowires for photocatalytic oxidation of acetone in air. *Chemosphere* **2007**, *66*, 2050-2057.
28. Yu, J.; Yu, J.C.; Leung, M.K.P.; Ho, W.; Cheng, B.; Zhao, X.; Zhao, J. Effects of acidic and basic hydrolysis catalysts on the photocatalytic activity and microstructures of bimodal mesoporous titania. *J. Catal.* **2003**, *217*, 69-78.
29. NIST Chemistry WebBook, NIST Standard Reference Database Number 69**,** Gaithersburg MD, 20899, Eds. P.J. Linstrom and W.G. Mallard, **2005**. Available online: http://webbook.nist.gov (accessed on 17 November 2020).
30. Behnajady, M. A.; Eskandarloo, H.; Modirshahla, N.; Shokri, M. Investigation of the effect of sol–gel synthesis variables on structural and photocatalytic properties of TiO_2 nanoparticles. *Desalination* **2011**, *278*, 10-17.
31. Becke, A. D. A new mixing of Hartree–Fock and local density-functional theories. *J. Chem. Phys.* **1993**, *98*, 1372-1377.
32. Stephens, P. J.; Devlin, F. J.; Chabalowski, C. F.; Frisch, M. J. Ab Initio Calculation of Vibrational Absorption and Circular Dichroism Spectra Using Density Functional Force Field. *J. Phys. Chem.* **1994**, *98*, 11623-11627.
33. Dunning Jr., T. H. Gaussian basis sets for use in correlated molecular calculations. I. The atoms boron through neon and hydrogen. *J. Chem. Phys.* **1989**, *90*, 1007-1023.
34. Kendall, R. A.; Dunning Jr., T. H.; Harrison, R. J. Electron affinities of the first-row atoms revisited. Systematic basis sets and wave functions. *J. Chem. Phys.* **1992**, *96*, 6796-6806.
35. Alagia, M.; Candori, P.; Falcinelli, S.; Pirani, F.; Pedrosa Mundim, M. S.; Richter, R.; Rosi, M.; Stranges, S.; Vecchiocattivi, F. Dissociative double photoionization of benzene molecules in the 26–33 eV energy range. *Phys. Chem. Chem. Phys.* **2011**, *13*, 8245-8250.
36. Alagia, M.; Balucani, N.; Candori, P.; Falcinelli, S.; Pirani, F.; Richter, R.; Rosi, M.; Stranges, S.; Vecchiocattivi, F. Production of ions at high energy and its role in extraterrestrial environments. *Rend. Lincei Sci. Fis. Nat.* **2013**, *24*, 53-65.
37. Skouteris, D.; Balucani, N.; Ceccarelli, C.; Faginas-Lago, N.; Codella, C.; Falcinelli, S.; Rosi, M. Interstellar dimethyl ether gas-phase formation: a quantum chemistry and kinetics study. *MNRAS* **2019**, *482*, 3567-3575.
38. Bartlett, R. J. Many-Body Perturbation Theory and Coupled Cluster Theory for Electron Correlation in Molecules. *Annu. Rev. Phys. Chem.* **1981**, *32*, 359-401.
39. Raghavachari, K.; Trucks, G. W.; Pople, J. A.; Head-Gordon, M. A fifth-order perturbation comparison of electron correlation theories. *Chem. Phys Lett.* **1989**, *157*, 479-483.
40. Olsen, J.; Jorgensen, P.; Koch, H.; Balkova, A.; Bartlett, R. J. Full configuration–interaction and state of the art correlation calculations on water in a valence double-zeta basis with polarization functions. *J. Chem. Phys.* **1996**, *104*, 8007-8015.
41. Frisch, M. J.; Trucks, G. W.; Schlegel, H. B.; Scuseria, G. E.; Robb, M. A.; Cheeseman, J. R.; Scalmani, G.; Barone, V.; Mennucci, B.; Petersson, G. A.; Nakatsuji, H.; Caricato, M.; Li, X.; Hratchian, H. P.; Izmaylov, A. F.; Bloino, J.; Zheng, G.; L. Sonnenberg, J.; Hada, M.; Ehara, M.; Toyota, K.; Fukuda, R.; Hasegawa, J.; Ishida, M.; Nakajima, T.; Honda, Y.; Kitao, O.; Nakai, H.; Vreven, T.; Montgomery, Jr., J. A.; Peralta, J. E.; Ogliaro, F.; Bearpark, M.; Heyd, J. J.; Brothers, E.; Kudin, K. N.; Staroverov, V. N.; Kobayashi, R.; Normand, J.; Raghavachari, K.; Rendell, A.; Burant, J. C.; Iyengar, S. S.; Tomasi, J.; Cosi, M.; Rega, N.; Milla, J. M.; Klene, M.; Knox, J. E.; Cross, J. B.; Bakken, V.; Adamo, C.; Jaramillo, J.; Gomperts, R.; Stratmann, R. E.; Yazyev, O.; Austin, A. J.; Cammi, R.; Pomelli, C.; Ochterski, J. W.; Martin, R. L.; Morokuma, K.; Zakrzewski,

V. G.; Voth, G. A.; Salvador, P.; Dannenberg, J. J.; Dapprich, S.; Daniels, A. D.; Farkas, O.; Foresman, J. B.; Ortiz, J. V.; Cioslowski, J.; Fox, D. J. Gaussian 09, Revision A.02, Gaussian, Inc., Wallingford CT **2009**.

42. Flükiger, P.; Lüthi, H. P.; Portmann, S.; Weber, J. *MOLEKEL 4.3*, Swiss Center for Scientific Computing, Manno (Switzerland) **2000-2002**.
43. Portmann, S. and Lüthi, H. P. MOLEKEL: an interactive molecular graphics tool. *Chimia* **2000**, *54*, 766-770.
44. Falcinelli, S.; Vecchiocattivi, F.; Pirani, F. General treatment for stereo-dynamics of state-to-state chemi-ionization reactions. *Commun. Chem.* **2020**, *3*, 64.
45. Falcinelli, S.; Farrar, J. M.; Vecchiocattivi, F.; Pirani, F. Quantum-State Controlled Reaction Channels in Chemi-ionization Processes: Radiative (Optical−Physical) and Exchange (Oxidative−Chemical) Mechanisms. *Acc. Chem. Res.* **2020**, *53(10)*, 2248-2260.